Catena 207 (2021) 105613

Contents lists available at ScienceDirect

Catena

journal homepage: www.elsevier.com/locate/catena

Soil depth-dependent C/N stoichiometry and fungal and bacterial communities along a temperate forest succession gradient

Zhen Bai [a,b,1], Ji Ye [a,1], Yu-Lian Wei [a], Shao-Kui Yan [b,*], Hai-Sheng Yuan [a,*]

[a] Chinese Academy of Sciences (CAS) Key Laboratory of Forest Ecology and Management, Institute of Applied Ecology, CAS, Shenyang 110164, China
[b] Hunan Key Laboratory for Structure and Ecosystem Service of Subtropical Forest, Huitong Hunan 418300, China

ARTICLE INFO

Keywords:
Bacteria
Fungi
High-throughput sequencing
C/N stoichiometry
Soil horizon
Forest succession

ABSTRACT

The vertical stratification of nutrient availability and related microbial adaptations in different soil horizons vary along forest succession gradients. However, the driving forces behind such age-related nutrient statuses and microbial dynamics and their depth-dependent distinctions remain unclear. To bridge these knowledge gaps, the current study investigated the carbon (C) and nitrogen (N) contents, C- and N-acquiring extracellular enzyme activities and fungal and bacterial communities in the organic layer (O), surface mineral soil (A) and mineral subsoil (B) in three temperate forest stands (35 years (y), 82 y and 200 y) in the Changbai Mountain region of northeastern China. The O-horizon presented age-related increasing C/N ratios as well as decreases in N%, enzyme (e.g., β-N-acetyl-glucosaminidase) activities and fungal and bacterial richness and diversity. In addition, the dominant early-stage (i.e., 35 y) O-horizon fungal and bacterial species presented positive relationships with the N content and copiotrophic characteristics, such as a powerful ability to mobilize available nutrients. However, the dominant late-stage (i.e., 200 y) O-horizon microbial species were negatively related to the N content but positively associated with the C content and/or C/N ratio and were characterized by an oligotrophic capacity for adapting to N deficiency and recalcitrant substrate decomposition. In the A- and B-horizons, however, the substrate availability (e.g., C and N contents) and nutrient cycling activities (e.g., enzyme activities and fungal and bacterial diversities) exhibited either a decreasing tendency from the early to the middle stage (i.e., 82 y) or an increasing tendency from the middle to the late stage. Such different or even opposing nutrient statuses and microbial adaptations between the decomposed organic matter and soil horizons suggest that the belowground biochemical characteristics are strongly determined by litter quality succession and microbial feedbacks to the depth-dependent allocation of available nutrients.

1. Introduction

Forest ecosystems fundamentally influence terrestrial element cycling and storage and their responses to climate-driven and human-induced environmental gradients (Bölscher et al., 2016; Creamer et al., 2016; Sasmito et al., 2020; Selmants et al., 2014). With forest succession, changes in dominant vegetation species (e.g., leaf litterfall and root exudates) can cause shifts in microbially-mediated decomposition and allocation of organic carbon (C) and nitrogen (N) compounds from the forest floor to mineral horizons (Brock et al., 2020; Currie et al., 1996; Luo et al., 2019; Vanderhoof et al., 2021). Thus, long-term consequences for tree community assembly present a gradient of ecosystem patterns and thus a chance to improve our knowledge on the edaphic traits (e.g., C/N stoichiometry) and biological activities (e.g., decomposers and enzymes) that predominate in organic matter decomposition and its depth-specific allocation (Schmidt et al., 2011). However, little is known about the mechanisms controlling belowground elemental stoichiometry and nutrient-acquiring microbial communities and their vertical stratification with forest development.

Across forest succession gradients, varying substrate availability is a driving force of microbial phylogenetic community assemblage and enzyme activities (e.g., β-glucosidase), leading to variations in nutrient sequestration in the soil beneath the litter horizon (Baldrian et al., 2008; Roy-Bolduc et al., 2015; Waring et al., 2016; Wu et al., 2013). Along a chronosequence of 5, 11, 21, and 30 years (y) post reforestation, microbial communities may shift from copiotrophic to oligotrophic

* Corresponding authors.
E-mail addresses: yanshaokui@cern.ac.cn (S.-K. Yan), hsyuan@iae.ac.cn (H.-S. Yuan).
[1] Equally contributed.

https://doi.org/10.1016/j.catena.2021.105613
Received 26 October 2020; Received in revised form 13 July 2021; Accepted 16 July 2021
Available online 24 July 2021

dominance, probably due to decreases in labile C and N substrates and accumulation of nutrient-poor and recalcitrant C components (Sun et al., 2017). As the humus horizon develops with forest stand succession, humicolous saprotrophs may be more active in decomposing organic substrates (Fernández-Toirán et al., 2006). Furthermore, fungal communities undergo more distinct changes than bacterial communities along forest succession gradients, as fungi have a stronger association with vegetation (e.g., plant symbioses and litter decomposers) and may outcompete bacteria in effectively utilizing root exudates and plant detritus (Sun et al., 2017; Zhong et al., 2018). Thus, strategy-dependent feedback in fungal communities is highly related to vegetation species and litter quality (e.g., leaf C/N ratio) (Roy-Bolduc et al., 2015; Wu et al., 2013), while bacterial community assemblage is more likely to be dependent upon edaphic properties (e.g., soil organic N) (Jiang et al., 2018). In addition, enzyme activities relating to organic matter turnover (e.g., N-acetyl-glucosaminidase) and litter decomposition are highly sensitive to inorganic N concentrations in early-successional forests (Allison et al., 2010). However, poor substrate quality (e.g., low N availability) at the late climax stage of forest succession may be associated with aggressive ectomycorrhizal fungal colonization and related enzyme activities, which decelerate litter decomposition (Waring et al., 2016). Thus, enzymatic degradation can be a rate-limiting step in the litter decomposition process and link microbial life strategies to changing elemental stoichiometry and substrate affinity in litter and upper soil horizons at different stages of vegetation succession (Schneider et al., 2012; Tischer et al., 2015; Voriskova and Baldrian, 2013).

Litter-derived compounds can be first immobilized by microorganisms in the upper forest floor and then in the subsoil (Guelland et al., 2013; Wang et al., 2020). Therefore, their biogeochemical transformations belowground are predicted to present marked depth stratification (Leinemann et al., 2018; Tripathi et al., 2013; Urbanová et al., 2015). Such top-down stratification effects are characteristic of decreasing microbial accessibility and substrate availability from upper to deeper horizons (Fuss et al., 2019; Kalks et al., 2020; Vormstein et al., 2020). With increasing soil depth, C/N enzymatic acquisition ratios decrease, suggesting that microbes adapt to requiring more energy in producing N- but not C-acquiring extracellular enzymes in metabolizing increasingly recalcitrant substrates in deeper soils (Zhou et al., 2020). Moreover, as litter substrate quality frequently varies with vegetation development, successional changes are always observed in belowground organic product allocation and depth-dependent nutrient-cycling processes (Bai et al., 2019; Blaško et al., 2015; Currie et al., 1996; Thuille and Schulze, 2006). Compared with old temperate coniferous forests, early-stage deciduous hardwood forests are characterized by higher rates of N cycling in litterfall and have greater vegetative N uptake and microbial N immobilization and organic C pools in mineral soils (DeLuca et al., 2002; Forstner et al., 2019; Guénon et al., 2017). However, in pine and pine-oak mixed stands (but not pure oak stands), the organic compound diversity and evenness can increase from the upper and less fragmented litter layer to the lower fragmented and humified horizon because of the accumulation of recalcitrant pine litter compounds and their decomposition products (Guénon et al., 2017).

A large area of natural temperate forests in Northeast China is located in the Changbai Mountain region, whose zonal climax vegetation is a broad-leaved Korean pine (*Pinus koraiensis*) mixed forest (averagely older than 200 y). Severe logging disturbances that occurred in the Second World War (1930s) and during industrialization (1980s) created naturally regenerated forests mainly composed of broadleaf *Betula platyphylla* and *Populus davidiana*. Thus, a human-induced forest succession gradient from the early pioneer to the late climax stage was formed over decades and constitutes a natural laboratory to explore edaphic and biotic drivers of element cycling and storage during forest development (Liang et al., 2018). By investigating the C/N stoichiometry, C- and N-targeting decomposition enzymes and the fungal and bacterial community compositions and richness in three horizons on a timescale of decades after high-severity deforestation, we aimed to address the following questions: 1) Are the nutrient availability and the microbial community composition and richness in the decomposed organic matter layer and mineral soil horizons closely related to forest succession stages? 2) Can horizon-specific shifts in nutrient cycling be explained by top-down stratification effects driven by microbial adaptation to varying litter quality during forest succession? We hypothesized that the distinct litter properties over the course of forest succession induce seral shifts in the substrate availability of decomposed organic matter and thereby change the microbially-mediated nutrient stratification across the upper soil and subsoil horizons.

2. Materials and methods

2.1. Site information and sample preparation

Sampling plots were located in the Changbai Mountain Natural Reserve (CMNR) of northeastern China (42°12-23'N; 128°0-13'E) (Fig. 1, Table 1). Precipitation occurs primarily from June to September and averages 700 mm annually; the annual average temperature is 2.8 °C (Yuan et al., 2016). The soil at the sampling site is an andosol that developed from volcanic ash (Bai et al., 2017). The young and middle succession stages of poplar-birch forests regenerated after forest logging in the CMNR in 1980 and 1933, respectively. In addition, although no Korean pine samplings occurred in the young succession stage, the middle succession stage encountered many saplings of Korean pine and thus showed a sign of forest succession from poplar-birch to broad-leaved Korean pine mixed forest. A broad-leaved Korean pine mixed forest with a mean forest age older than 200 y, which is the typical zonal climax vegetation in the CMNR (Liang et al., 2018; Zhang et al., 2015), was regarded as a late succession stage. Samples were collected from July 5 to 9, 2015. The succession stages were therefore denoted as 35 y, 82 y and 200 y, respectively.

In each forest stand, ten plots (15 m × 15 m each) were randomly chosen as sample replicates, and the minimum distance between two plots was approximately 50 m. The ten replicates for each forest stand should be considered pseudoreplicates. A total of five subsamples were mixed to yield a composite sample for each plot. Before the sampling of each plot, collection materials were sterilized with 70% alcohol. Samples were collected separately for the horizons of intermediately to highly decomposed organic matter (Oa + Oe according to the SUDA soil taxonomy, i.e., O), surface mineral soil (A) (ca. 0–5 cm depth) and mineral subsoil (B) (ca. 5–10 cm), which provide an opportunity to explore the temporal patterns of depth-dependent C/N stoichiometry and microbial communities during forest development in the CMNR of northeastern China. The samples were transported at 4 °C and sieved through a 2-mm mesh to remove visible roots and rocks. Then, the samples were stored at −80 °C for DNA extraction, lyophilized for enzyme activity determination or air-dried at room temperature for one week for chemical analyses.

2.2. C/N stoichiometry and enzyme activity analyses

The dried soil samples were sieved through a 100 mesh screen for the detection of C and N contents with an elemental analyzer (Elementar Vario Macro, Germany). Extracellular enzyme activities were detected via high-throughput fluorometric measurement using 96-well microplates as reported by Bell et al. (2013) and He et al. (2016) with slight modification. β-N-acetyl-glucosaminidase (NAG) activity is closely related to the mineralization of N-containing compounds (e.g., chitin and peptidoglycan), whereas the other enzymes depolymerize carbohydrate biopolymers such as cellulose (β-D-cellobiohydrolase, CBH; β-1,4-glucosidase, BG), starch (α-1,4-glucosidase, AG) and hemicelluloses (β-xylosidase, XYL) (Bell et al., 2013; Tischer et al., 2015; Zhao et al., 2018). A 2-gram aliquot of the soil sample was suspended in 200 mL of 1 mmol L^{-1} NaN_3 (to inhibit the growth of microbes) in a

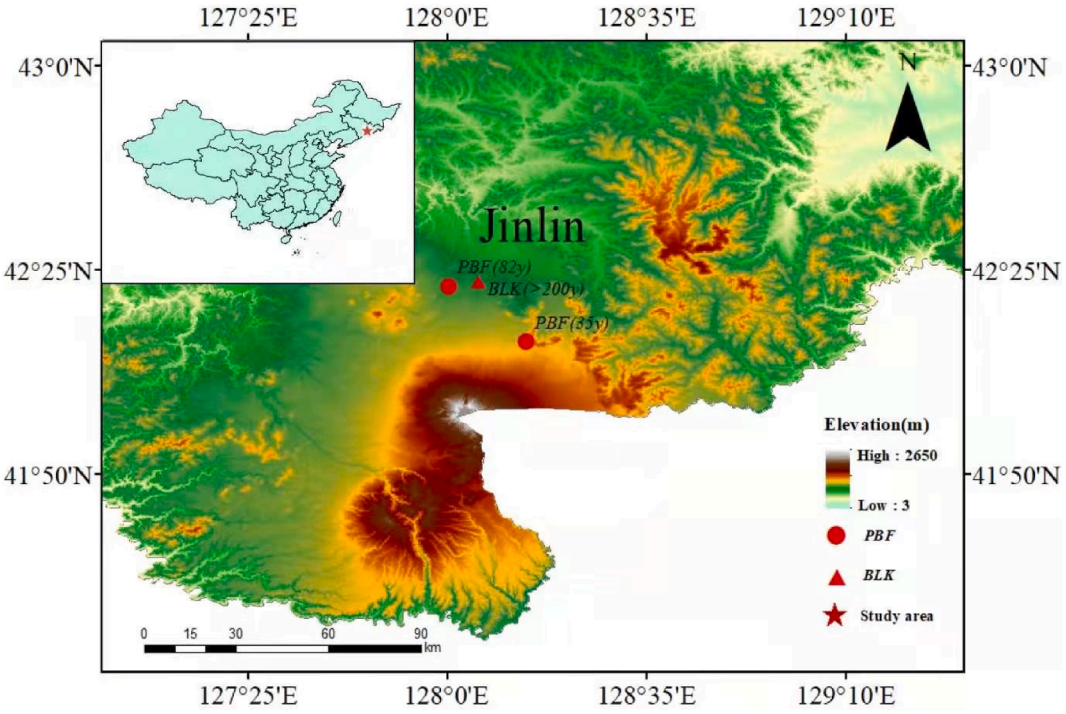

Fig. 1. The localization of investigated sites. The PBF and BLK study sites are poplar-birch forest and broad-leaved Korean pine mixed forest, respectively.

Table 1
Characteristics of sampling sites.

Stand age	Forest type	Longitude	Latitude	Altitude (m)
35 y	Poplar-birch forest	128°13′59″ E	42°12′41″ N	1129
82 y	Poplar-birch forest	128°00′18″ E	42°22′ 17″ N	860
>200 y	Broad-leaved Korean pine mixed forest	128°05′ 31″ E	42°23′ 05″ N	800

blender for 15 min. Then, 100 μl of the soil slurry was mixed with 100 μl of 200 μmol MUB-linked substrates and 50 μl of modified universal buffer. Additional 4-methylumbelliferone (MUB) standards (0–100 μmol/L concentrations) were included with each sample. There was a control microplate where the soil slurry was replaced by 100 μl of 1 mmol L^{-1} NaN_3. Sample and control microplates were incubated at 25 °C for 4 h. The substrates of the tested enzyme included 4-methylumbelliferyl N-acetyl-β-D-glucosaminide for NAG, 4-methylumbelliferyl α-D-glucopyranoside for AG, 4-methylumbelliferyl β-D-glucopyranoside for BG, 4-methylumbelliferyl β-D-cellobiopyranoside for CBH, and 4-methylumbelliferyl β-D-xylopyranoside for XYL. Then, 250 μl of the supernatants were pipetted into black and flat-bottomed 96-well plates to detect the fluorescence and absorbance intensities via an Infinite 200 Pro spectrophotometer (Tecan, Switzerland). Fluorescence measurements were conducted at wavelengths of 365 nm (excitation) and 450 nm (emission).

2.3. DNA extraction and sequencing

Genomic DNA was extracted from 0.5 g of soil with a PowerSoil DNA Isolation Kit (MoBio Laboratories, USA), and its concentration and A260/280 ratio were detected with a NanoDrop 2000 UV–Vis spectrophotometer (Thermo Fisher Scientific Inc., USA). The internal transcribed spacer (ITS) sequence forward primer ITS3-2024F (5′-GCATCGATGAAGAACGCAGC-3′) and reverse primer ITS4-2409R (5′-TCCTCCGCTTATTGATATGC-3′) with a unique barcode were used to amplify the ITS2 region (Bellemain et al., 2010; Maza-Marquez et al., 2018). The universal primers 515F (5′-GTGCCAGCMGCCGCGGTAA-3′) and 907R (5′-CCGTCAATTCCTTTGAGTTT-3′) with a unique barcode were used for the V4-V5 region of bacterial 16S rRNA gene amplification (Knelman et al., 2017; Tischer et al., 2015; Yang et al., 2007). The PCR (25 μl) consisted of 5–10 ng of total DNA, 1 unit of Ex Taq (TaKaRa, Dalian, China), 1 × Ex Taq buffer, 0.2 mmol of each dNTP and 0.4 μmol of each primer. Fungal amplification conditions consisted of an initial denaturation step of 94 °C for 5 min, followed by 30 cycles of 94 °C for 30 s, 53 °C for 30 s and 72 °C for 50 s with a final extension at 72 °C for 5 min. Bacterial amplification conditions were as follows: 94 °C for 3 min, followed by 30 cycles of denaturation at 94 °C for 40 s, annealing at 56 °C for 60 s, extension at 72 °C for 60 s, and a final extension at 72 °C. Replicate PCRs were carried out for each sample, and their products were pooled and subjected to 1% agarose gel electrophoresis. The band with the correct size was excised and purified using a SanPrep DNA Gel Extraction Kit (Sangon Biotech, Shanghai, China). All PCR products were quantified with a NanoDrop and pooled with equimolar amounts of each sample. Sequencing libraries were generated using the Ion Plus Fragment Library Kit 48 rxns (Thermo Fisher Scientific Inc., USA) following the manufacturer's recommendations. Library quality was assessed on a Qubit 2.0 fluorometer (Thermo Fisher Scientific Inc., USA). The library was then sequenced on an Ion S5™ XL platform, and single-end reads were generated.

2.4. Analysis of high-throughput sequencing data

Single-end reads were trimmed and assigned to each sample based on their unique barcodes. Quality filtering of the raw reads was performed according to Cutadapt (Buresova et al., 2019) (Version 1.9.1, http://cutadapt.readthedocs.io/en/stable/). Sequences were clustered into operational taxonomic units (OTUs) using the cd-hit clustering algorithm (Li and Godzik, 2006) at a 97% threshold pairwise identity with *pick_otus.py* (QIIME, version 1.7.0). Singletons and doubletons were removed during OTU selection. The aligned sequences were inspected for chimeras using the UCHIME algorithm (Edgar et al., 2011). The taxonomic classification for each prokaryotic OTU was carried out using the Ribosomal Database

Project (RDP) Classifier against the Greengenes 16S rRNA database with a minimum confidence of 0.8 (Wang et al., 2007), while the fungal taxonomy was assigned against the UNITE reference database in version 7.0 (Kõljalg et al., 2013). All samples were normalized to the smallest sample size (40,894 and 58,690 reads/sample for bacteria and fungi, respectively). Diversity analyses were performed by running a workflow in QIIME. The complexity of microbial species diversity for each sample was assessed based upon the abundance-based indexes of observed species, diversity (Shannon) and evenness (Simpson). Among these diversity indexes, the Shannon and Simpson indexes are sensitive to rare species abundance (Banerjee et al., 2016). Sequences were deposited in the NCBI Sequence Read Archive under accession number SUB6787713.

2.5. Statistical analyses

One-way ANOVA (Tukey's honestly significant difference (HSD) test) was used to assess differences in normally distributed data (Shapiro-Wilk test); otherwise, we conducted Kruskal-Wallis test via the Boxplerk function in R software (R Development Core Team, 2019, version 3.6.1). Constrained correspondence analysis (CCA) was performed with fungal and bacterial OTUs (>0.5% relative abundance) using the vegan package of R based on the length of the gradient along the first ordination axis (Bai et al., 2019; Schostag et al., 2015). Figures were constructed using Origin 9.0 (OriginLab Corp., USA). As previously reported (Bai et al., 2020), the key fungal and bacterial species were clustered into 9 groups (three stand ages × three horizons) based on the Spearman correlation coefficients of the individual species in each group (Figs. SI-1, SI-2).

3. Results

3.1. C/N stoichiometry

In the O-horizon, the C content had no difference between 35 y and 82 y (42–43%) but significantly increased to 45% at 200 y ($P < 0.05$, Fig. 2A); the N content was 2% at 35 y and declined by 13% to 82 y and by 37% to 200 y (Fig. 2D). Thus, the C/N ratio was 22 at 35 y and increased by 14% to 82 y and by 68% to 200 y (Fig. 2G). In the A- and B-horizons, the C and N contents were generally lowest at 82 y. Compared to the early and/or late succession stage(s), the middle-stage C contents declined 13–20% in the A-horizon and 31–32% in the B-horizon (Fig. 2B, 2C); the middle-stage N contents decreased 16% in the A-horizon from 35 y to 82 y and 36% in the B-horizon from 200 y to 82 y (Fig. 2F). The A- and B-horizon C/N ratios decreased 6% and 18%, respectively, from 35 y to 82 y (Fig. 2H, 2I). Furthermore, the C/N stoichiometry was strongly affected by horizon effects: from the O- to the B-horizon, the C and N contents decreased 70–90% (Fig. 2A-F); the C/N ratios decreased by 37%, 55% and 68% at 35 y, 82 y and 200 y, respectively (Fig. 2G-I).

3.2. Enzyme activities

In the O-horizon, the AG and BG activities were highest at 35 y but had no difference between 82 y and 200 y (Fig. 3D, 3G); the XYL activities decreased 21% from 35 y to 82 y and 29% from 82 y to 200 y (Fig. 3M); in contrast, the CBH activities increased approximately 1.2-fold from 35 y to later succession stages (Fig. 3J). In the A- and B-horizons, most of the enzyme activities significantly decreased from 35 y to 82 y but tended to increase from 82 y to 200 y (Fig. 3). Moreover, the

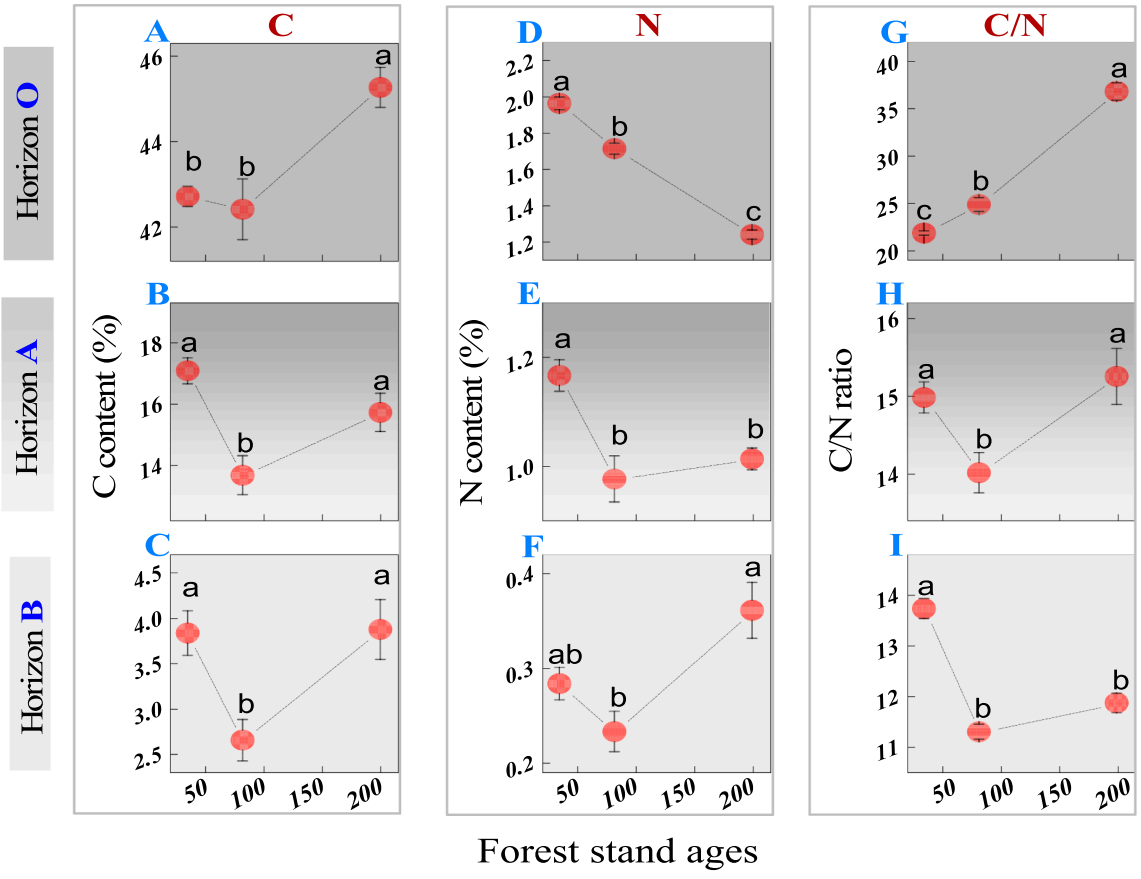

Fig. 2. Litter and soil C/N stoichiometry in different soil horizons along the forest succession gradient; (A-C) carbon (C) contents in the O-, A- and B-horizons; (D-F) nitrogen (N) contents in the O-, A- and B-horizons; (G-I) C/N ratios in the O-, A- and B-horizons. Values are shown as the means and standard errors (N = 10). Different letters indicate significant differences at $P < 0.05$.

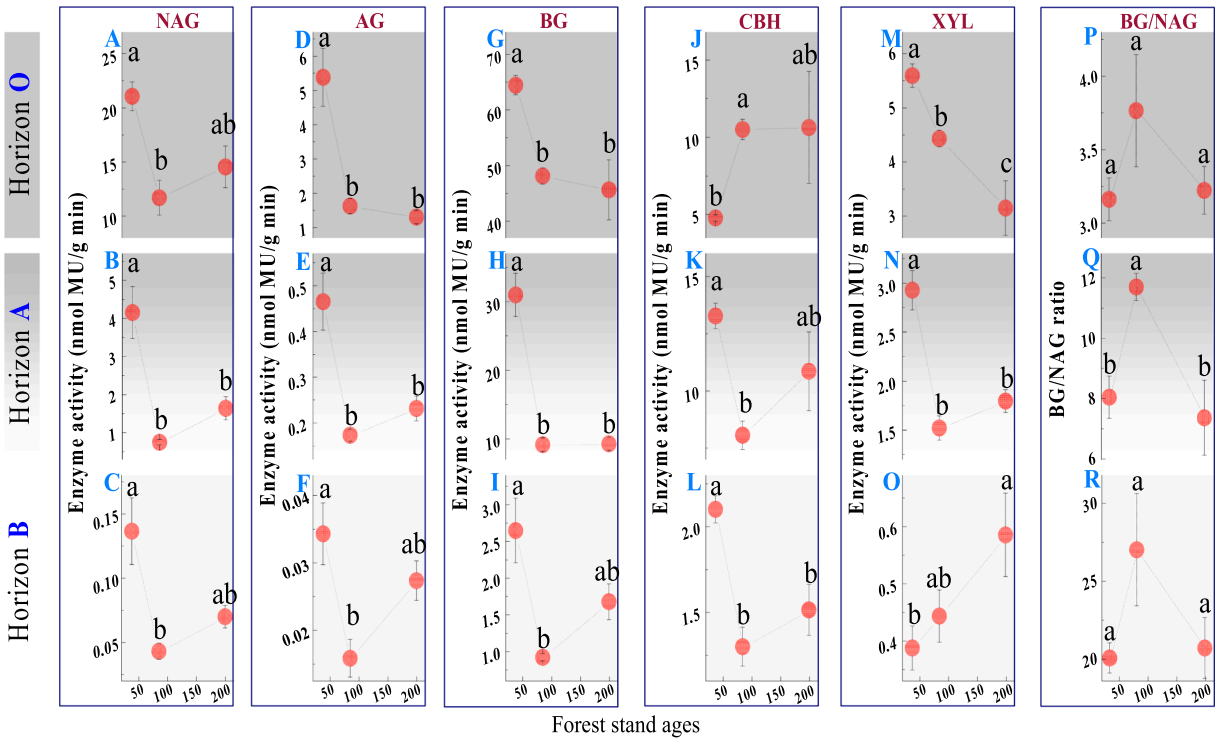

Fig. 3. Enzyme activities in different soil horizons along the forest succession gradient; (A-C) β-N-acetyl glucosaminidase (NAG) activities in the O-, A- and B-horizons; (D-F) α-1,4-glucosidase (AG) activities in the O-, A- and B-horizons; (G-I) β-1,4-glucosidase (BG) activities in the O-, A- and B-horizons; (J-L) β-D-cellobiohydrolase (CBH) activities in the O-, A- and B-horizons; (M-O) β-xylosidase (XYL) activities in the O-, A- and B-horizons; (P-R) BG/NAG ratio in the O-, A- and B-horizons. Values are shown as the means and standard errors (N = 10). Different letters indicate significant differences at $P < 0.05$.

XYL activities in the B-horizon continuously increased 51% from 35 y to 200 y (Fig. 3O). For horizon effects, the NAG activities presented pronounced horizon differentiation and decreased by more than 99% from the O- to the B-horizon (Fig. 3A-C); in contrast, the CBH activities varied little between the O- and A-horizons and decreased by a minimum of 56% from the O- to the B-horizon (Fig. 3J-L).

3.3. Fungal and bacterial richness, diversity and evenness

Compared to that at 35–82 y, the microbial diversity at 200 y generally decreased in the O-horizon but increased in the A- and B-horizons (Figs. 4, 5). Specifically, the O-horizon bacterial observed species, Shannon index and Simpson index decreased by 58%, 26% and 4%, respectively, from 35 y to 200 y (Fig. 5A, 5D, 5G). In contrast, the A-horizon fungal observed species increased by 20% from 35 y to 200 y (Fig. 4B). The variation in horizon effects differed between fungal and bacterial richness: the number of fungal species (except for 200 y) decreased 32–39% from the O- to the B-horizon (Fig. 4A, 4C); however, the numbers of bacterial species were 23–69% higher in the A-horizon than in the O- and B-horizons (Fig. 5A-C).

3.4. Fungal and bacterial community compositions

As shown in Fig. 6A and 7A, the fungal and bacterial community compositions of subsamples were first grouped according to horizon and then strongly influenced by stand age. The 9 groups of fungi and bacteria were distinctly distributed along and significantly influenced by horizon and stand age (Figs. 4, 5).

3.4.1. Fungal community

As Fig. 6 and Table SI-1 show, the O-horizon and mineral soil horizons were frequently abundant in G1-2 and G9 species and in G3-8 species, respectively. Compared to that at 35–82 y, the O-horizon at 200 y was less abundant in G9 species but significantly increased in terms of certain G2 species (e.g., *D. glomerata*, *G. baccata* and *P. cucumerina*). The A-horizon presented negative aging trends with respect to G6 (e.g., *T. harzianum*) and G9 (e.g., *M. alpina*) but was most abundant in G4 (e.g., *M. humilis*) and G7 (e.g., *G. applanatum* and *S. terricola*) at 200 y. The B-horizon showed negative aging effects with respect to G3 species but positive aging effects for G7 species. Furthermore, the most abundant species in the A- and B-horizons at 82 y was *T. asperum* (G8), with relative abundances of 6–16%.

3.4.2. Bacterial community

As shown in Fig. 7 and Table SI-2, the O-, A- and B-horizons were abundant in G1-2 species, G9 species and G4-6 species, respectively. Compared to that at 35–82 y, the O-horizon at 200 y had significantly higher abundances of G1 species but lower abundances of G2-4 species. In the A- and/or B-horizon, positive aging effects were observed with respect to G8 species; in contrast, the late stage (200 y) had less abundant G4 (e.g., *Burkholderia* sp.).

4. Discussion

4.1. Aging effects

Our C/N stoichiometry values for the O-horizon and mineral soil horizons are within the ranges of previously reported C (37–45%) and N contents (<2.0%) and C/N ratios (12–36) (Bai et al., 2019; Papa et al., 2014; Zheng et al., 2018). The age-related decreasing N% but increasing C/N ratio in the O-horizon (Fig. 2D, 2G) strongly suggest that N deficiency becomes more constrained along with forest succession (Blaško et al., 2015; Sun et al., 2017). Reduced N availability inhibits enzyme activities (Allison et al., 2010; Schneider et al., 2012), slows nutrient cycling (Brunn et al., 2016), and negatively influences microbial diversity (Zhao et al., 2019). Accordingly, the current seral tendency of the O-horizon C/N stoichiometry (Fig. 2D, 2G) was accompanied by age-related decreases in enzyme activities (e.g., Fig. 3M) and microbial

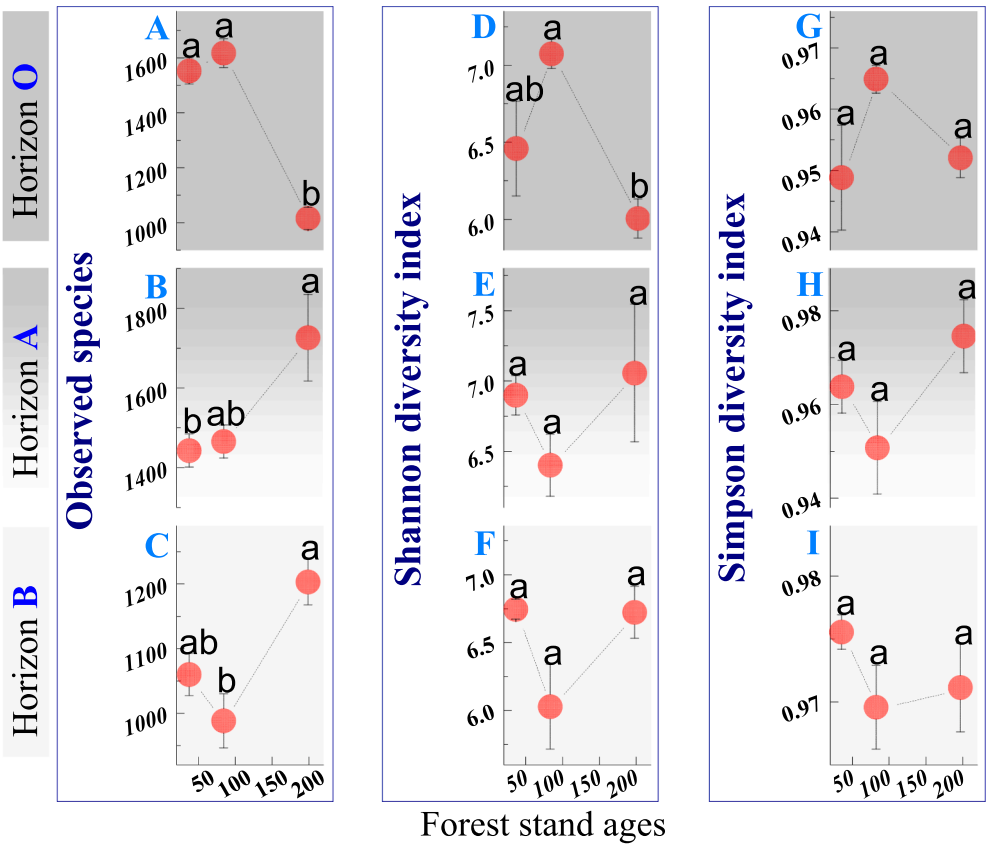

Fig. 4. Fungal richness, diversity and evenness in different soil horizons along the forest succession gradient; (A-C) the number of species in the O-, A- and B-horizons; (D-F) Shannon index in the O-, A- and B-horizons; (G-I) Simpson index in the O-, A- and B-horizons. Values are shown as the means and standard errors (N = 10). Different letters indicate significant differences at $P < 0.05$.

richness, diversity and evenness (e.g., Fig. 5A, 5D, 5G).

The early-stage O-horizon dominant species of fungi (e.g., *M. hiemalis* in G9, Fig. 6B) and bacteria (e.g., *Burkholderia* sp. and *D. japonica* in G4, Fig. 7B) were all significantly and positively related to the N content and enzyme activities (Tables 2 and 3). These species are capable of releasing weathering-active organic acids and extracellular enzymes to powerfully hydrolyze C polymers and rapidly immobilize available nutrients (Brunner et al., 2011; Deacon et al., 2006; Rincón-Molina et al., 2020; Schisler et al., 2019). Their close associations with high N availability and nutrient cycling strongly suggest their copiotrophic life strategies (Cline and Zak, 2015; Siles and Margesin, 2016; Zhang et al., 2018).

In contrast, the late-stage O-horizon dominant species of fungi (e.g., *D. glomerata*, *G. baccata* and *P. cucumerina* in G2, Fig. 6B) and bacteria (e.g., *F. pectinovorum*, *R. cellulosilyticum*, *S. rhizophila* and *C. soldanellicola* in G1, Fig. 7B) were negatively related to the N content and enzyme activities but positively related to the C content and/or C/N ratio (Tables 2-3). Moreover, these species can decompose cellulosic remains and grow on natural leaves or wood as the sole C source (Carles et al., 2018; Garcia-Fraile et al., 2007; Yang et al., 2014) and may be stimulated to preferably utilize lignocellulosic polymers as N availability declines (Currey et al., 2010; Guénon et al., 2017; Zhang et al., 2008). Thus, the O-horizon CBH activities increased in the late stage (Fig. 3J). Together, the major late-stage litter decomposers adapted to low nutrient-cycling activity and complex substrate decomposition processes, which being closely related to an oligotrophic lifestyle.

T. asperum was predominant in the A- and B-horizons of the middle-stage (Fig. 6B). This species can produce large amounts of NAG in hydrolyzing N-acetylglucosamine of fungal chitin and bacterial peptidoglycan (Tischer et al., 2015). Therefore, it has a high potential to utilize recalcitrant complex substrates and to promote the reutilization of microbial residues (Poll et al., 2010; Semenov et al., 1996). In addition, the A- and/or B-horizon at 82 y had the lowest C and N contents (Fig. 2B-C, 2E-F), enzyme activities (e.g., Fig. 3B-C, 3E-F), and fungal and bacterial diversities (e.g., Fig. 4C, 5F) but the highest BG/NAG ratio (e.g., Fig. 3Q-R). All these findings suggest that the mineral soil horizons had been experiencing the strongest nutrient constraints and the lowest cycling activities and an extremely urgent demand for N availability at 82 y. Soil available N was also severely depleted from young to middle-aged stands of Chinese fir due to enhanced organic N utilization by rapidly increasing aboveground production and mineral N acquisition by soil microbial groups (Zhang et al., 2019).

Furthermore, the late-stage dominant species in the A- and/or B-horizon (Fig. 6B, 7B) can 1) use phosphonate derivatives by cleaving C-N and C-phosphorus (P) bonds (e.g., the fungi *M. humilis* (G4) and *S. terricola* (G7)) (Stosiek et al., 2019; Tanney and Hutchison, 2010) and 2) degrade plant residues (e.g., fungi such as *G. applanatum* (G7) (Beets et al., 2008) and bacteria such as *S. jaspsi* (G8) (Asker et al., 2007; Chung et al., 2011), *L. soli* (G8) (Jeon et al., 2016) and *Unid. Gammaproteobacteria* (G9) (Johnsen et al., 2002; Kumar et al., 2018)). Together with having the highest fungal richness (Fig. 4B) and bacterial diversity and evenness (Fig. 5E, 5H), the late-stage soil horizons should tend to harbor diversified microbial communities that were screened for powerfully decomposing complex substrates but not rapidly consuming labile nutrients. Thus, no further N depletion was exhibited in the upper mineral soil horizon, and N accumulation even occurred in the subsoil horizon (Fig. 2E-F). Dissolved nutrient (e.g., N) concentrations and fluxes in mineral soil were also observed to be much higher in old coniferous forests than in young hardwood stands, probably due to stronger microbial immobilization processes (e.g., the formation of recalcitrant polyphenol-organic-N complexes derived from pine litter) and lower vegetation uptake in coniferous forests than in hardwood forests (Currie

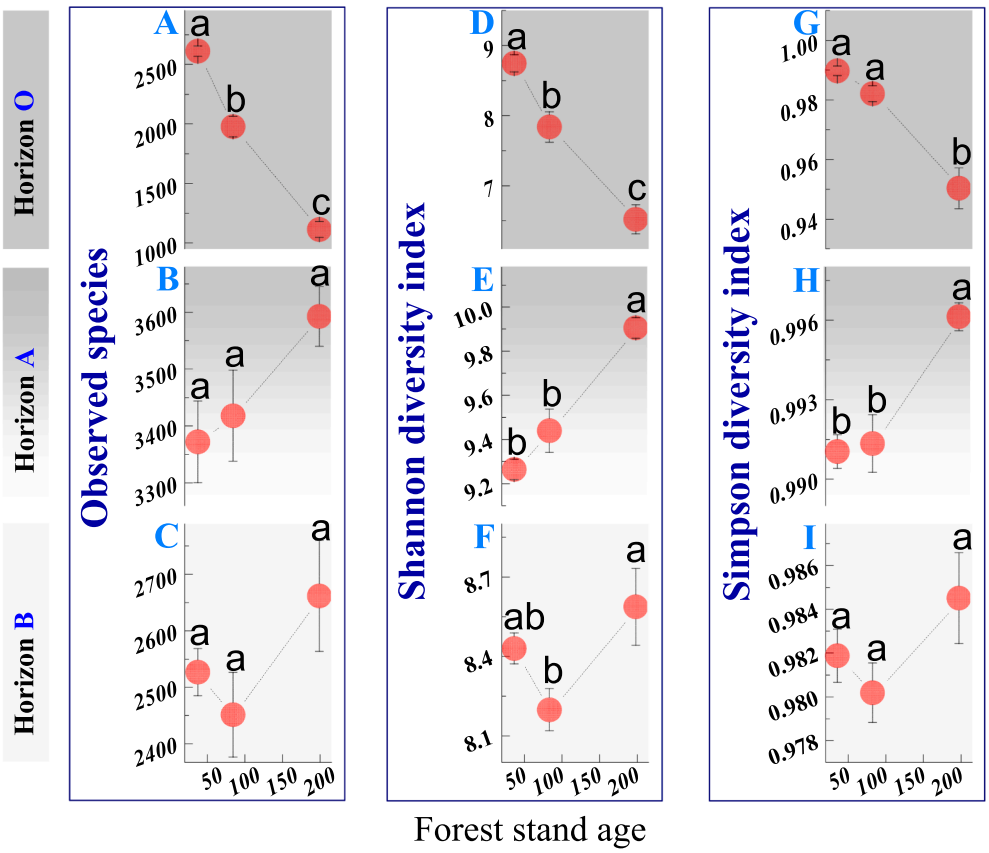

Fig. 5. Bacterial richness, diversity and evenness in different soil horizons along the forest succession gradient; (A-C) the number of species in the O-, A- and B-horizons; (D-F) Shannon index in the O-, A- and B-horizons; (G-I) Simpson index in the O-, A- and B-horizons. Values are shown as the means and standard errors (N = 10). Different letters indicate significant differences at $P < 0.05$.

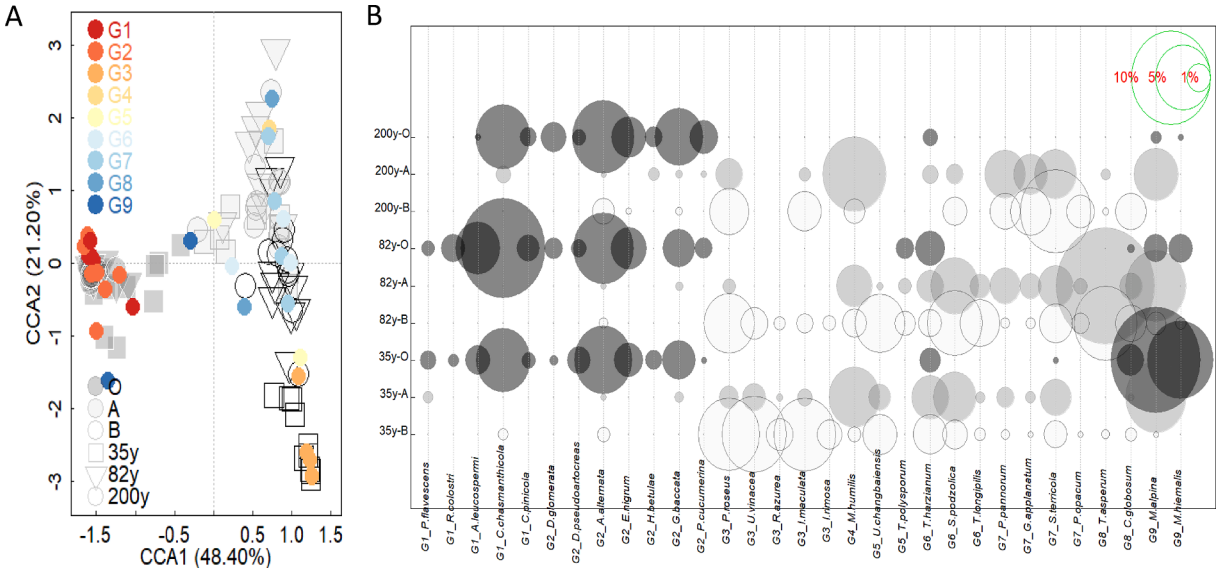

Fig. 6. Constrained correspondence analysis (CCA) and relative abundances of fungal OTUs (>0.5%). In the CCA (A), the forest stand ages are separately denoted as circles (200 y), triangles pointing downward (82 y) and squares (35 y); the subsamples of horizons are graphically displayed as black (i.e., O-horizon), light gray (i.e., A-horizon) and white (i.e., B-horizon). In the bubble map of the relative abundances of key species (B), the O-horizon is displayed in black, the A-horizon in gray and the B-horizon in white.

et al., 1996; DeLuca et al., 2002; Guénon et al., 2017).

4.2. Horizon effects

Plant detritus is strongly decomposed by cellulolytic and ligninolytic enzymes (Frey et al., 2004), which are mainly produced by fungal

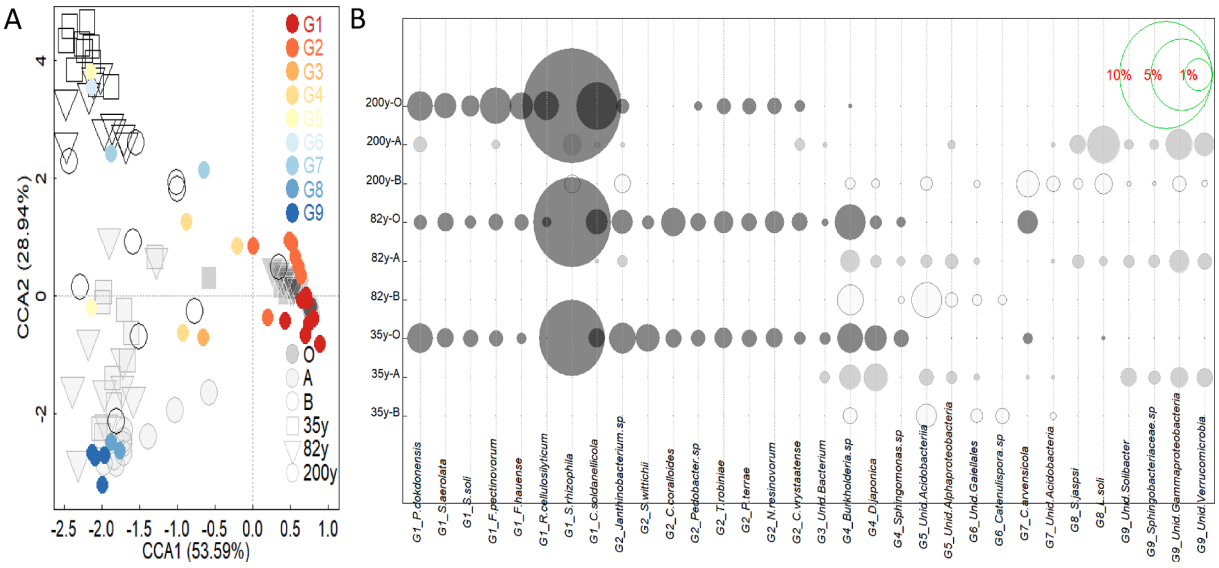

Fig. 7. Constrained correspondence analysis (CCA) and relative abundances of bacterial OTUs (>0.5%). In the CCA (A), the forest stand ages are separately denoted as circles (200 y), triangles pointing downward (82 y) and squares (35 y); the subsamples of horizons are graphically displayed in black (i.e., O-horizon), light gray (i.e., A-horizon) and white (i.e., B-horizon). In the bubble map for the relative abundances of key species (B), the O-horizon is displayed in black, the A-horizon in gray and the B-horizon in white.

Table 2
Kendall tau correlation coefficients between fungal community diversity and key species and C/N stoichiometry and enzyme activity. BG, β-1,4-glucosidase; NAG, β-N-acetyl-glucosaminidase; AG, α-1,4-glucosidase; XYL, β-xylosidase; CBH, β-D-cellobiohydrolase. Species without any significant correlation with C/N and enzymes were removed. Values in bold denote statistical significance ($P < 0.05$).

	Indexes and species	N	C	C/N	BG	NAG	AG	XYL	CBH
O	Observed_species	**0.36**	**−0.44**	**−0.40**	0.25	0.10	**0.35**	**0.38**	0.01
O	Shannon	0.12	**−0.27**	−0.16	0.08	0.00	0.18	**0.26**	0.10
O	G1_*P.flavescens*	**0.30**	**−0.30**	**−0.39**	**0.27**	0.04	0.24	**0.32**	−0.11
O	G1_*R.colostri*	0.01	**−0.32**	−0.09	−0.10	−0.11	0.06	0.13	0.18
O	G1_*A.leucospermi*	0.22	**−0.34**	**−0.27**	0.05	−0.11	0.16	0.22	0.16
O	G1_*C.chasmanthicola*	−0.03	−0.13	−0.03	−0.06	−0.20	−0.03	0.08	**0.32**
O	G2_*D.glomerata*	**−0.31**	0.01	**0.26**	**−0.42**	**−0.33**	**−0.32**	**−0.33**	0.11
O	G2_*D.pseudoartocreas*	**0.26**	−0.12	**−0.32**	0.18	0.09	**0.32**	**0.27**	**−0.37**
O	G2_*E.nigrum*	−0.14	−0.15	0.04	**−0.26**	**−0.37**	−0.21	−0.21	−0.09
O	G2_*H.betulae*	−0.04	0.08	0.03	0.11	0.17	0.11	−0.01	**−0.32**
O	G2_*G.baccata*	**−0.27**	0.23	**0.28**	−0.22	−0.22	**−0.32**	**−0.35**	0.04
O	G2_*P.cucumerina*	**−0.49**	**0.31**	**0.46**	**−0.40**	−0.19	**−0.37**	**−0.46**	0.04
O	G5_*T.polysporum*	0.06	**−0.35**	−0.13	−0.04	**−0.32**	−0.22	−0.02	0.14
O	G9_*M.alpina*	**0.39**	−0.01	**−0.35**	0.10	0.04	0.19	0.10	−0.15
O	G9_*M.hiemalis*	**0.50**	−0.12	**−0.48**	**0.34**	0.20	**0.39**	**0.46**	**−0.29**
A	G3_*I.maculata*	0.10	0.24	0.21	0.20	**0.35**	**0.31**	**0.28**	**0.32**
A	G5_*U.changbaiensis*	**0.29**	0.16	0.05	**0.33**	**0.35**	**0.30**	**0.35**	**0.29**
A	G6_*T.harzianum*	**0.27**	0.16	0.02	0.13	0.16	0.07	0.14	0.06
A	G7_*P.pannorum*	−0.25	−0.06	0.11	**−0.32**	−0.20	**−0.31**	**−0.31**	−0.19
A	G7_*G.applanatum*	**−0.27**	−0.15	0.04	**−0.37**	−0.18	**−0.27**	**−0.30**	−0.18
A	G7_*S.terricola*	−0.10	−0.07	0.02	−0.18	−0.07	−0.18	−0.10	−0.02
A	G8_*T.asperum*	**−0.38**	**−0.36**	−0.19	−0.23	**−0.44**	**−0.36**	**−0.35**	**−0.41**
A	G9_*M.alpina*	0.18	−0.04	**−0.27**	0.08	−0.12	0.02	0.03	−0.07
B	Observed_species	**0.38**	**0.27**	0.11	0.22	0.14	**0.26**	0.20	0.10
B	Shannon	**0.33**	0.24	0.19	**0.31**	0.14	**0.32**	0.09	**0.26**
B	Simpson	0.20	0.09	0.23	**0.28**	0.18	**0.32**	−0.05	**0.26**
B	G3_*U.vinacea*	−0.10	0.09	**0.44**	**0.33**	**0.27**	0.15	−0.14	**0.36**
B	G3_*R.azurea*	−0.06	0.12	**0.31**	**0.31**	**0.37**	0.24	−0.13	**0.38**
B	G3_*I.maculata*	−0.09	0.11	**0.34**	**0.27**	**0.41**	0.09	−0.11	**0.35**
B	G3_*I.rimosa*	−0.19	−0.01	0.20	0.20	0.22	0.10	−0.09	**0.27**
B	G4_*M.humilis*	0.03	−0.09	−0.21	**−0.26**	−0.21	−0.22	0.11	−0.25
B	G6_*S.podzolica*	**−0.31**	**−0.44**	**−0.28**	**−0.39**	**−0.37**	**−0.29**	−0.13	**−0.35**
B	G6_*T.longipilis*	−0.22	−0.25	−0.21	**−0.33**	**−0.32**	**−0.32**	0.01	**−0.26**
B	G7_*P.pannorum*	**0.35**	0.21	−0.09	0.13	0.07	**0.27**	0.23	−0.02
B	G7_*G.applanatum*	**0.34**	0.16	−0.11	0.03	0.01	0.15	0.24	−0.10
B	G7_*S.terricola*	**0.27**	0.09	−0.24	−0.13	−0.10	−0.03	0.25	−0.23
B	G7_*P.opacum*	0.23	0.02	−0.25	−0.16	**−0.31**	−0.13	0.18	**−0.34**
B	G8_*T.asperum*	−0.21	**−0.35**	**−0.30**	**−0.32**	**−0.43**	**−0.32**	−0.03	**−0.35**

Table 3
Kendall tau correlation coefficients between bacterial community diversity and key species and C/N stoichiometry and enzyme activity. BG, β-1,4-glucosidase; NAG, β-N-acetyl-glucosaminidase; AG, α-1,4-glucosidase; XYL, β-xylosidase; CBH, β-D-cellobiohydrolase. Species without any significant correlation with C/N and enzyme were removed. Values in bold denote statistical significance ($P < 0.05$).

	Indexes and species	N	C	C/N	BG	NAG	AG	XYL	CBH
O	Observed_species	**0.68**	−0.25	**−0.62**	**0.52**	**0.37**	**0.64**	**0.63**	−0.24
O	Shannon	**0.53**	−0.22	**−0.45**	**0.45**	**0.33**	**0.53**	**0.49**	−0.20
O	Simpson	**0.51**	−0.24	**−0.43**	**0.43**	**0.32**	**0.47**	**0.46**	−0.15
O	G1_*P.dokdonensis*	−0.07	**0.31**	0.11	0.12	**0.31**	0.07	−0.05	−0.08
O	G1_*S.aerolata*	**−0.32**	**0.40**	**0.33**	−0.03	0.04	−0.18	−0.19	0.14
O	G1_*S.soli*	−0.14	**0.43**	0.23	0.06	0.22	−0.02	−0.10	0.10
O	G1_*F.pectinovorum*	**−0.33**	**0.45**	**0.32**	−0.15	−0.06	−0.23	**−0.27**	0.18
O	G1_*F.hauense*	**−0.51**	**0.40**	**0.49**	−0.21	−0.14	**−0.45**	**−0.35**	**0.33**
O	G1_*R.cellulosilyticum*	**−0.53**	**0.27**	**0.49**	**−0.42**	**−0.28**	**−0.56**	**−0.59**	0.09
O	G1_*S.rhizophila*	**−0.41**	0.25	**0.32**	**−0.32**	**−0.28**	**−0.31**	**−0.33**	0.14
O	G1_*C.soldanellicola*	**−0.48**	**0.30**	**0.42**	**−0.35**	**−0.33**	**−0.48**	**−0.50**	0.19
O	G2_*Janthinobacterium* sp.	**0.40**	−0.07	**−0.35**	**0.39**	**0.32**	**0.40**	**0.39**	−0.12
O	G2_*S.wittichii*	**0.55**	−0.20	**−0.56**	**0.41**	**0.35**	**0.51**	**0.50**	**−0.29**
O	G2_*C.coralloides*	**0.27**	**−0.48**	**−0.32**	0.01	−0.14	0.13	0.16	0.18
O	G2_*Pedobacter* sp.	**0.31**	**−0.27**	**−0.31**	0.17	−0.01	0.17	0.12	0.03
O	G2_*N.resinovorum*	0.21	**−0.29**	**−0.26**	0.12	−0.08	0.07	0.15	−0.07
O	G2_*C.vrystaatense*	0.08	−0.19	−0.15	−0.07	**−0.33**	−0.21	−0.08	−0.14
O	G3_*Unid.Bacterium*	**0.43**	**−0.33**	**−0.35**	0.25	**0.26**	**0.40**	**0.27**	−0.15
O	G4_*Burkholderia* sp.	**0.31**	**−0.43**	**−0.36**	0.20	0.07	**0.31**	**0.35**	0.07
O	G4_*D.japonica*	**0.46**	**−0.40**	**−0.47**	**0.35**	0.21	**0.45**	**0.44**	−0.04
O	G4_*Sphingomonas* sp.	**0.26**	−0.08	−0.24	**0.26**	**0.31**	**0.33**	**0.41**	−0.05
O	G7_*C.arvensicola*	0.21	**−0.35**	−0.24	0.07	−0.11	0.07	0.16	0.12
A	Shannon	**−0.34**	−0.12	0.13	**−0.26**	−0.12	−0.13	**−0.27**	−0.14
A	Simpson	−0.25	−0.09	0.19	−0.25	−0.12	−0.12	−0.25	−0.12
A	G3_*Unid.Bacterium*	0.15	**0.27**	0.13	**0.27**	0.24	**0.30**	0.25	**0.26**
A	G4_*Burkholderia* sp.	**0.28**	0.11	−0.07	**0.29**	0.18	0.12	0.19	0.10
A	G4_*D.japonica*	**0.40**	**0.28**	0.14	**0.58**	**0.49**	**0.47**	**0.42**	**0.43**
A	G5_*Unid.Acidobacteriia*	**0.30**	0.08	−0.10	**0.31**	0.17	0.12	0.25	0.07
A	G8_*S.jaspsi*	**−0.34**	−0.24	0.07	**−0.37**	−0.25	**−0.34**	**−0.35**	**−0.28**
A	G8_*L.soli*	**−0.29**	−0.12	0.16	**−0.39**	−0.16	−0.17	**−0.26**	−0.11
A	G9_*Unid.Solibacter*	**0.27**	**0.28**	0.12	**0.42**	**0.38**	**0.42**	**0.46**	**0.43**
A	G9_*Sphingobacteriaceae* sp.	0.08	−0.16	**−0.28**	0.12	−0.08	0.10	0.07	−0.04
B	Observed_species	0.15	0.20	0.02	0.22	0.19	**0.26**	0.01	0.17
B	Shannon	0.22	**0.37**	0.12	**0.37**	**0.39**	**0.35**	0.23	**0.30**
B	G4_*Burkholderia* sp.	−0.14	−0.10	−0.20	−0.18	−0.23	**−0.27**	0.11	−0.16
B	G5_*Unid.Acidobacteriia*	**−0.32**	−0.25	−0.06	−0.24	−0.21	**−0.30**	−0.11	−0.08
B	G5_*Unid.Alphaproteobacteria*	−0.24	**−0.32**	**−0.48**	**−0.40**	**−0.45**	**−0.39**	0.09	**−0.40**
B	G9_*Unid.Gammaproteobacteria*	**0.48**	**0.37**	−0.17	**0.32**	0.15	0.23	**0.54**	0.02

communities (Papa et al., 2014). Accordingly, in the O-horizon, cellulolytic enzyme activities (e.g., AG and/or XYL) were significantly positively related to fungal richness and diversity (Table 2). The fungal species (e.g., *M. alpina* and *M. hiemalis* (G9)) (Fig. 6B) are dominant in the early-stage O-horizon, as they are common decomposers of fresh poplar and birch litter (Jayasinghe and Parkinson, 2008; Osono and Takeda, 2007). Notably, the O-horizon bacterial richness, diversity, evenness, and dominant species (e.g., *Janthinobacterium* and *S. wittichii* (G2), *D. japonica* and *Sphingomonas* sp. (G4), Fig. 7B) were significantly positively related to the N% and enzyme activities (except for CBH, Table 3), which were all higher at the early stage than at the late stage (e.g., Fig. 2D, 3D, 5A). Litter decomposition is generally dominated by fungi rather than bacteria and the extracellular enzymes required for litter decomposition are mostly produced by fungi but not bacteria (Romaní et al., 2006; Schneider et al., 2012). However, strong positive relationships between bacterial abundance and enzyme activities can be observed due to bacterial "cheating behavior" (i.e., use of simple compounds released through fungal decomposition) (Romaní et al., 2006; Schneider et al., 2012). It is likely that copiotrophic bacterial consortia preferentially acquire metabolites during fungal-dominant litter decomposition at the early-stage O-horizon. In addition, although bacteria are believed to be dependent upon fungal enzymatic activity and intermediate litter decomposition products, stimulated bacteria can prosper by inhibiting fungal growth through the release of lytic agents/antibiotics and competition for the available organic compounds (Romaní et al., 2006).

The A-horizon-specific/dominant bacteria (e.g., *Burkholderia* sp. and *D. japonica* in G4, Fig. 7B) have great potential to promote atmospheric N fixation (Fonseca et al., 2018; Lardi et al., 2017; Muresu et al., 2011; Palaniappan et al., 2010) and solubilize inorganic P and thus increase P availability (e.g., *Burkholderia* sp.) (Zhou et al., 2018). As nutrient-cycling activities were positively correlated with the abovementioned species but weakly or negatively correlated with bacterial diversity and evenness indexes (Table 3), the nutrient-cycling processes in the A-horizon should be closely constrained by functional groups specialized in N fixation or P exploitation but not by colonizers responsible for acquiring readily available organic C and N.

The dominant microbial species in the B-horizon (e.g., the fungi *P. roseus* (G3) and *S. terricola* (G7), Fig. 6B) can excrete extracellular enzymes to directly cleave C-N-P bonds to use organic derivatives as sole nutrient sources (Kwaśna, 2004; Kwaśna et al., 2016; Stosiek et al., 2019). They can dominate in the metabolization of chitin and cellulose under anaerobic conditions (e.g., the fungi *U. vinacea* (G3) and *U. changbaiensis* (G5) in Fig. 6B; bacteria such as *Catenulispora* sp. (G6) and *C. arvensicola* (G7) in Fig. 7B) (Busti et al., 2006; Fisk et al., 2011; Khusnullina et al., 2018; Kolton et al., 2011; Sukdeo et al., 2018). These results, together with the depth-dependent variations either to a greater extent for NAG activities (Fig. 3A-C) or to a lesser extent for CBH activities (Fig. 3J-L), suggest that the B-horizon is characterized by deep-layer metabolism of recalcitrant and N-deficient residual compounds. In addition, the consistently contrasting tendencies of N content (Fig. 2D vs. 2F), XYL activity (Fig. 3M vs. 3O) and fungal diversity (Fig. 4A vs. 4C) between the O- and B-horizons probably reflected that the initial fungal decomposers of accessible hemicellulose components are

strongly dependent on N status and driven by the top-down transport of litter decomposition products (Brabcová et al., 2018; DeAngelis et al., 2011; Stone et al., 2012). The fungal and bacterial diversities were positively related to the C and N contents and enzyme activities (Tables 2 and 3), suggesting that B-horizon microbial groups are well adapted to the pulse transfer of readily available metabolites that are likely translocated from the upper horizons.

4.3. Vertical stratification driven by seral shifts in litter quality

In the current study, differences or even inverse relationships frequently occurred between the decomposed organic matter and mineral soil horizons in terms of C/N stoichiometry (Fig. 2D-F, 2G-I), enzyme activities related to C and N cycling (Fig. 3J-L, 3M-O), microbial richness, diversity and evenness (e.g., Fig. 4A-C), and microbial community compositions (Figs. 6, 7). In particular, N content 1) exhibited an age-related decrease in the O-horizon (Fig. 2D), 2) did not differ between 82 y and 200 y in the A-horizon (Fig. 2E), and 3) significantly increased from 82 y to 200 y in the B-horizon (Fig. 2F).

Although the vegetation type was similar between 35 y and 82 y, diminished N availability can occur due to greater N acquisition along with rapid development and an increase in the size of broadleaf forests (Idol et al., 2003; Sheng et al., 2017; Zhang and Wang, 2012; Zhu et al., 2012). As a result, despite no difference in the C% (Fig. 2A), the O-horizon experienced a decline in the N% from 35 y to 82 y (Fig. 2D). During the earlier succession stages (35–82 y), the O-horizon was characteristic of high levels of substrate quality (e.g., high N% in Fig. 2D, low C/N ratio in Fig. 2G), enzyme activities (e.g., XYL in Fig. 3M) and bacterial richness and diversity (Fig. 5A, 5D) and thus copiotrophic life strategies. All of these results suggest a high probability of rapid sequestration of the labile nutrients in the decomposed litter horizon and low leaching of the available metabolites to the A- and B-horizons. Therefore, nutrient-cycling succession and the vertical stratification of available C occurred concurrently across the upper soil and subsoil horizons from 35 y to 82 y, i.e., 20% and 31% declines in the A- and B-horizons, respectively (Fig. 2B-C). The seral C/N stoichiometry distinction at 35–82 y was amplified so much with increasing soil depth that contrasting C/N ratio trends occurred between the O-horizon (35 y $<$ 82 y) and the corresponding underlying soil horizons (35 y $>$ 82 y) (Fig. 2G, 2I).

Interestingly, compared to 35–82 y, the microbial diversity at 200 y was lower in the O-horizon but generally higher in the underlying soil horizons (e.g., Fig. 4A-C, 5D-E). In the O-horizon, recalcitrant residuals accumulate along with forest succession; hence, slow-growing species breaking down more recalcitrant compounds tend to be selected for and enriched at late stage (McGee et al., 2019). Such increased oligotrophic growth leads to the slow consumption of available residues and prevents the rapid depletion of soluble nutrients (Blaško et al., 2015; Nara, 2006), leading to a high probability of the vertical distribution of labile nutrients (Nara et al., 2003). Moreover, late-stage coniferous litter input, which is associated with highly recalcitrant compounds and complicated decomposition processes, can contribute greatly to the diversity and evenness of organic compounds (Guénon et al., 2017). Thus, the A- and B-horizons accumulated diverse and readily available organic C derived from plant detritus. Furthermore, as mentioned above, coniferous forests take up less N from soil than broadleaf forests (Currie et al., 1996). Accordingly, at 82–200 y, the A-horizon did not further decrease in N% (Fig. 2E) and even increased in bacterial evenness (Fig. 5H); moreover, there were increases in C% and N% (Fig. 2C, 2F), enzyme activities (e.g., Fig. 3O), and microbial richness and diversity (e.g., Fig. 4C, 5F) in the B-horizon. The replacement of certain dominant microbial species also acted as ecosystem-level feedback. For instance, A-horizon copiotrophic bacteria (e.g., *Burkholderia* sp. and *D. japonica* (G4), Fig. 7B) were depleted to a greater extent at the late stage (i.e., 200 y) than at the earlier stages (i.e., 35–82 y), probably due to decreased bioavailable organic C in the upper soil horizon that had directly leached from the litter horizon (Leinemann et al., 2018). The fungi *U. changbaiensis* (G5) and *T. harzianum* (G6) (Fig. 6B), which are more relevant to recalcitrant components than to readily hydrolyzable carbohydrates (Osono et al., 2006), were absent from the B-horizon at 200 y. Together, the above-mentioned successional distinctions between horizons can be explained by multiple top-down sieving processes, i.e., vertical stratification of nutrient availability is first determined by the substrate preference of microbial trophic lifestyle at organic matter layer and is then driven by microbial adaptation to the corresponding underlying translocation of decomposition products at mineral soil horizons.

5. Conclusions

The distinct or even contrasting seral shifts in microbial community composition and diversity and nutrient cycling (e.g., C, N, and enzyme activities) between the decomposed organic matter and mineral soil horizons shown here clearly confirm our hypothesis that changes in decomposing litter quality with forest succession influence organic nutrient availability and microbial community diversity and structure in the upper soil and subsoil. We speculate that the distinct seral nutrient-cycling processes between the decomposed organic matter horizon and the upper soil and subsoil horizons can be explained by top-down "sieving effects", which are strongly determined by the long-term strategy-dependent evolution of microbial groups in response to nutrient acquisition in the soil profile. Such close associations between microbial adaptations and the biochemical composition of organic matter (e.g., C/N stoichiometry) can be important selective forces that control the age-related nutrient status and depth-dependent microbial feedback strategies in forest ecosystems (Schmidt et al., 2011).

Declaration of Competing Interest

The authors declare that they have no known competing financial interests or personal relationships that could have appeared to influence the work reported in this paper.

Acknowledgments

This work was supported by the National Key Research and Development Program of China (2016YFC0500301), the Hunan Key Laboratory for Structure and Ecosystem Service of Subtropical Forest (2018htf002) and the National Natural Science Foundation of China (31870018).

Appendix A. Supplementary material

Supplementary data to this article can be found online at https://doi.org/10.1016/j.catena.2021.105613.

References

Allison, S.D., Gartner, T.B., Mack, M.C., McGuire, K., Treseder, K., 2010. Nitrogen alters carbon dynamics during early succession in boreal forest. Soil Biol. Biochem. 42 (7), 1157–1164.

Asker, D., Beppu, T., Ueda, K., 2007. Sphingomonas jaspsi sp. nov., a novel carotenoid-producing bacterium isolated from Misasa, Tottori, Japan. Int. J. Syst. Evol. Microbiol. 57, 1435–1441.

Bölscher, T., Wadsö, L., Börjesson, G., Herrmann, A.M., 2016. Differences in substrate use efficiency: impacts of microbial community composition, land use management, and substrate complexity. Biol. Fertil. Soils 52 (4), 547–559.

Bai, Z., Ma, Q., Dai, Y., Yuan, H., Ye, J.i., Yu, W., 2017. Spatial heterogeneity of SOM concentrations associated with white-rot versus brown-rot wood decay. Sci. Rep. 7 (1) https://doi.org/10.1038/s41598-017-14181-7.

Bai, Z., Wu, X., Lin, J.-J., Xie, H.-T., Yuan, H.-S., Liang, C., 2019. Litter-, soil- and C:N-stoichiometry-associated shifts in fungal communities along a subtropical forest succession. Catena 178, 350–358.

Bai, Z., Yuan, Z.-Q., Wang, D.-M., Fang, S., Ye, J.i., Wang, X.-G., Yuan, H.-S., 2020. Ectomycorrhizal fungus-associated determinants jointly reflect ecological processes in a temperature broad-leaved mixed forest. Sci. Total Environ. 703, 135475. https://doi.org/10.1016/j.scitotenv.2019.135475.

Baldrian, P., Trögl, J., Frouz, J., Šnajdr, J., Valášková, V., Merhautová, V., Cajthaml, T., Herinková, J., 2008. Enzyme activities and microbial biomass in topsoil layer during

spontaneous succession in spoil heaps after brown coal mining. Soil Biol. Biochem. 40 (9), 2107–2115.
Banerjee, S., Baah-Acheamfour, M., Carlyle, C.N., Bissett, A., Richardson, A.E., Siddique, T., Bork, E.W., Chang, S.X., 2016. Determinants of bacterial communities in Canadian agroforestry systems. Environ. Microbiol. 18 (6), 1805–1816.
Beets, P.N., Hood, I.A., Kimberley, M.O., Oliver, G.R., Pearce, S.H., Gardner, J.F., 2008. Coarse woody debris decay rates for seven indigenous tree species in the central North Island of New Zealand. For. Ecol. Manage. 256 (4), 548–557.
Bell, C.W., Fricks, B.E., Rocca, J.D., Steinweg, J.M., McMahon, S.K., Wallenstein, M.D., 2013. High-throughput fluorometric measurement of potential soil extracellular enzyme activities. J. Vis. Exp. (81) https://doi.org/10.3791/50961.
Bellemain, E., Carlsen, T., Brochmann, C., Coissac, E., Taberlet, P., Kauserud, H., 2010. ITS as an environmental DNA barcode for fungi: an in silico approach reveals potential PCR biases. BMC Microbiol. 10 (1), 189. https://doi.org/10.1186/1471-2180-10-189.
Blaško, R., Holm Bach, L., Yarwood, S.A., Trumbore, S.E., Högberg, P., Högberg, M.N., 2015. Shifts in soil microbial community structure, nitrogen cycling and the concomitant declining N availability in ageing primary boreal forest ecosystems. Soil Biol. Biochem. 91, 200–211.
Brabcová, V., Štursová, M., Baldrian, P., 2018. Nutrient content affects the turnover of fungal biomass in forest topsoil and the composition of associated microbial communities. Soil Biol. Biochem. 118, 187–198.
Brock, O., Kalbitz, K., Absalah, S., Jansen, B., 2020. Effects of development stage on organic matter transformation in Podzols. Geoderma 378, 114625. https://doi.org/10.1016/j.geoderma.2020.114625.
Brunn, M., Condron, L., Wells, A., Spielvogel, S., Oelmann, Y., 2016. Vertical distribution of carbon and nitrogen stable isotope ratios in topsoils across a temperate rainforest dune chronosequence in New Zealand. Biogeochemistry 129 (1-2), 37–51.
Brunner, I. et al., 2011. Pioneering fungi from the Damma glacier forefield in the Swiss Alps can promote granite weathering. Geobiology, 9, 266-79.
Buresova, A., Kopecky, J., Hrdinkova, V., Kamenik, Z., Omelka, M., Sagova-Mareckova, M., Vieille, C., 2019. Succession of microbial decomposers is determined by litter type, but site conditions drive decomposition rates. Appl. Environ. Microbiol. 85 (24) https://doi.org/10.1128/AEM.01760-19.
Busti, E. et al., 2006. Catenulispora acidiphila gen. nov., sp. nov., a novel, mycelium-forming actinomycete, and proposal of Catenulisporaceae fam. nov. Int. J. Syst. Evol. Microbiol., 56, 1741–6.
Carles, L., Rossi, F., Besse-Hoggan, P., Blavignac, C., Leremboure, M., Artigas, J., Batisson, I., 2018. Nicosulfuron degradation by an ascomycete fungus isolated from submerged Alnus Leaf Litter. Front Microbiol. 9 https://doi.org/10.3389/fmicb.2018.0316710.3389/fmicb.2018.03167.s001.
Chung, E.J. et al., 2011. Sphingomonas oryziterrae sp. nov. and Sphingomonas jinjuensis sp. nov. isolated from rhizosphere soil of rice (Oryza sativa L.). Int J Syst Evol Microbiol, 61, 2389-94.
Cline, L.C., Zak, D.R., 2015. Soil microbial communities are shaped by plant-driven changes in resource availability during secondary succession. Ecology 96 (12), 3374–3385.
Creamer, R.E., et al., 2016. Ecological network analysis reveals the inter-connection between soil biodiversity and ecosystem function as affected by land use across Europe. Appl. Soil Ecol. 97, 112–124.
Currey, P.M. et al., 2009. Turnover of labile and recalcitrant soil carbon differ in response to nitrate and ammonium deposition in an ombrotrophic peatland. Global Change Biology, 16, 2307–2321.
Currie, W.S., Aber, J.D., McDowell, W.H., Boone, R.D., Magill, A.H., 1996. Vertical transport of dissolved organic C and N under long-term N amendments in pine and hardwood forests. Biogeochemistry 35 (3), 471–505.
Deacon, L.J., Janie Pryce-Miller, E., Frankland, J.C., Bainbridge, B.W., Moore, P.D., Robinson, C.H., 2006. Diversity and function of decomposer fungi from a grassland soil. Soil Biol. Biochem. 38 (1), 7–20.
DeAngelis, K.M. et al., 2011. Characterization of trapped lignin-degrading microbes in tropical forest soil. PLoS One, 6, e19306.
DeLuca, T., Nilsson, M.-C., Zackrisson, O., 2002. Nitrogen mineralization and phenol accumulation along a fire chronosequence in northern Sweden. Oecologia 133 (2), 206–214.
Edgar, R.C., Haas, B.J., Clemente, J.C., Quince, C., Knight, R., 2011. UCHIME improves sensitivity and speed of chimera detection. Bioinformatics, 27, 2194-200.
Fernández-Toirán, L.M., Ágreda, T., Olano, J.M., 2006. Stand age and sampling year effect on the fungal fruit body community in *Pinus pinaster* forests in central Spain. Can. J. Bot. 84 (8), 1249–1258.
Fisk, M.C., Fahey, T.J., Sobieraj, J.H., Staniec, A.C., Crist, T.O., 2011. Rhizosphere disturbance influences fungal colonization and community development on dead fine roots. Plant Soil 341 (1-2), 279–293.
Fonseca, E.d.S., Peixoto, R.S., Rosado, A.S., Balieiro, F.d.C., Tiedje, J.M., Rachid, C.T.C.d.C., 2018. The microbiome of eucalyptus roots under different management conditions and its potential for biological nitrogen fixation. Microb. Ecol. 75 (1), 183–191.
Forstner, S.J., Wechselberger, V., Müller, S., Keibinger, K.M., Díaz-Pinés, E., Wanek, W., Scheppi, P., Hagedorn, F., Gundersen, P., Tatzber, M., Gerzabek, M.H., Zechmeister-Boltenstern, S., 2019. Vertical redistribution of soil organic carbon pools after twenty years of nitrogen addition in two temperate coniferous forests. Ecosystems 22 (2), 379–400.
Frey, S.D., Knorr, M., Parrent, J.L., Simpson, R.T., 2004. Chronic nitrogen enrichment affects the structure and function of the soil microbial community in temperate hardwood and pine forests. For. Ecol. Manage. 196 (1), 159–171.
Fuss, C.B., Lovett, G.M., Goodale, C.L., Ollinger, S.V., Lang, A.K., Ouimette, A.P., 2019. Retention of nitrate-N in mineral soil organic matter in different forest age classes. Ecosystems 22 (6), 1280–1294.
Garcia-Fraile, P. et al., 2007. Rhizobium cellulosilyticum sp. nov., isolated from sawdust of Populus alba. Int J Syst Evol Microbiol, 57, 844-8.
Guénon, R., Day, T.A., Velazco-Ayuso, S., Gros, R., 2017. Mixing of Aleppo pine and Holm oak litter increases biochemical diversity and alleviates N limitations of microbial activity. Soil Biol. Biochem. 105, 216–226.
Guelland, K., Esperschütz, J., Bornhauser, D., Bernasconi, S.M., Kretzschmar, R., Hagedorn, F., 2013. Mineralisation and leaching of C from 13C labelled plant litter along an initial soil chronosequence of a glacier forefield. Soil Biol. Biochem. 57, 237–247.
He, F., Yang, B., Wang, H., Yan, Q., Cao, Y., He, X., 2016. Changes in composition and diversity of fungal communities along Quercus mongolica forests developments in Northeast China. Appl. Soil Ecol. 100, 162–171.
Idol, T.W., Pope, P.E., Ponder, F., 2003. N mineralization, nitrification, and N uptake across a 100-year chronosequence of upland hardwood forests. For. Ecol. Manage. 176 (1-3), 509–518.
Jayasinghe, B.A.T.D., Parkinson, D., 2008. Actinomycetes as antagonists of litter decomposer fungi. Appl. Soil Ecol. 38 (2), 109–118.
Jeon, H.J., Kim, M.-N., Park, E.-S., 2016. Thermal, mechanical and biodegradation properties of pure, epoxidized and methoxylated castor oil based polyurethane. Plast., Rubber Compos. 45 (1), 1–8.
Jiang, Y., Lei, Y., Yang, Y., Korpelainen, H., Niinemets, Ü., Li, C., 2018. Divergent assemblage patterns and driving forces for bacterial and fungal communities along a glacier forefield chronosequence. Soil Biol. Biochem. 118, 207–216.
Johnsen, A.R., Winding, A., Karlson, U., Roslev, P., 2002. Linking of microorganisms to phenanthrene metabolism in soil by analysis of (13)C-labeled cell lipids. Appl Environ Microbiol 68 (12), 6106–6113.
Kõljalg, U., Nilsson, R.H., Abarenkov, K., Tedersoo, L., Taylor, A.F.S., Bahram, M., Bates, S.T., Bruns, T.D., Bengtsson-Palme, J., Callaghan, T.M., Douglas, B., Drenkhan, T., Eberhardt, U., Dueñas, M., Grebenc, T., Griffith, G.W., Hartmann, M., Kirk, P.M., Kohout, P., Larsson, E., Lindahl, B.D., Lücking, R., Martín, M.P., Matheny, P.B., Nguyen, N.H., Niskanen, T., Oja, J., Peay, K.G., Peintner, U., Peterson, M., Põldmaa, K., Saag, L., Saar, I., Schüßler, A., Scott, J.A., Senés, C., Smith, M.E., Suija, A., Taylor, D.L., Telleria, M.T., Weiss, M., Larsson, K.-H., 2013. Towards a unified paradigm for sequence-based identification of fungi. Mol. Ecol. Notes 22 (21), 5271–5277.
Kalks, F., Liebmann, P., Wordell-Dietrich, P., Guggenberger, G., Kalbitz, K., Mikutta, R., Helfrich, M., Don, A., 2020. Fate and stability of dissolved organic carbon in topsoils and subsoils under beech forests. Biogeochemistry 148 (2), 111–128.
Khusnullina, A.I., Bilanenko, E.N., Kurakov, A.V., 2018. Microscopic fungi of white sea sediments. Contemporary Probl. Ecol. 11 (5), 503–513.
Knelman, J., Graham, E., Ferrenberg, S., Lecoeuvre, A., Labrado, A., Darcy, J., Nemergut, D., Schmidt, S., 2017. Rapid shifts in soil nutrients and decomposition enzyme activity in early succession following forest fire. Forests 8 (9), 347. https://doi.org/10.3390/f8090347.
Kolton, M., Meller Harel, Y., Pasternak, Z., Graber, E.R., Elad, Y., Cytryn, E., 2011. Impact of biochar application to soil on the root-associated bacterial community structure of fully developed greenhouse pepper plants. Appl. Environ. Microbiol. 77 (14), 4924–4930.
Kumar, M., et al., 2018. Genomic and proteomic analysis of lignin degrading and polyhydroxyalkanoate accumulating beta-proteobacterium Pandoraea sp. ISTKB. Biotechnol Biofuels 11, 154.
Kwaśna, H., 2004. Natural shifts in communities of rhizosphere fungi of common oak after felling. Plant Soil 264 (1/2), 209–218.
Kwaśna, H., Małecka, M., Sierota, Z., Jaworski, T., 2016. Effects of sawdust amendment on forest soil fungal community and infestation by cockchafers. Dendrobiology 75, 87–97.
Lardi, M., de Campos, S.B., Purtschert, G., Eberl, L., Pessi, G., 2017. Competition experiments for legume infection identify burkholderia phymatum as a highly competitive beta-rhizobium. Front. Microbiol. 8, 1527.
Leinemann, T., Preusser, S., Mikutta, R., Kalbitz, K., Cerli, C., Höschen, C., Mueller, C.W., Kandeler, E., Guggenberger, G., 2018. Multiple exchange processes on mineral surfaces control the transport of dissolved organic matter through soil profiles. Soil Biol. Biochem. 118, 79–90.
Li, W., Godzik, A., 2006. Cd-hit: a fast program for clustering and comparing large sets of protein or nucleotide sequences. Bioinformatics 22 (13), 1658–1659.
Liang, X., Liu, S., Wang, H., Wang, J., 2018. Variation of carbon and nitrogen stoichiometry along a chronosequence of natural temperate forest in northeastern China. Journal of Plant Ecology, 11, 339-350.
Luo, X., Hou, E., Zhang, L., Zang, X., Yi, Y., Zhang, G., Wen, D., 2019. Effects of forest conversion on carbon-degrading enzyme activities in subtropical China. Sci. Total Environ. 696, 133968. https://doi.org/10.1016/j.scitotenv.2019.133968.
Maza-Márquez, P., Vílchez-Vargas, R., González-Martínez, A., González-López, J., Rodelas, B., 2018. Assessing the abundance of fungal populations in a full-scale membrane bioreactor (MBR) treating urban wastewater by using quantitative PCR (qPCR). J. Environ. Manage. 223, 1–8.
McGee, K.M., Eaton, W.D., Shokralla, S., Hajibabaei, M., 2019. Determinants of soil bacterial and fungal community composition toward carbon-use efficiency across primary and secondary forests in a Costa Rican conservation area. Microb. Ecol. 77 (1), 148–167.
Muresu, R., Polone, E., Sorbolini, S., Squartini, A., 2011. Characterization of endophytic and symbiotic bacteria within plants of the endemic associationCentaureetum horridaeMol. Plant Biosystems – Int. J. Dealing Aspects Plant Biol. 145 (2), 478–484.

Nara, K., 2006. Ectomycorrhizal networks and seedling establishment during early primary succession. New Phytol. 169 (1), 169–178.
Nara, K., Nakaya, H., Hogetsu, T., 2003. Ectomycorrhizal sporocarp succession and production during early primary succession on Mount Fuji. New Phytol. 158 (1), 193–206.
Osono, T., Hirose, D., Fujimaki, R., 2006. Fungal colonization as affected by litter depth and decomposition stage of needle litter. Soil Biol. Biochem. 38 (9), 2743–2752.
Osono, T., Takeda, H., 2007. Microfungi associated with Abies needles and Betula leaf litter in a subalpine coniferous forest. Can. J. Microbiol. 53 (1), 1–7.
Palaniappan, P., Chauhan, P.S., Saravanan, V.S., Anandham, R., Sa, T., 2010. Isolation and characterization of plant growth promoting endophytic bacterial isolates from root nodule of Lespedeza sp. Biol. Fertil. Soils 46 (8), 807–816.
Papa, S., Cembrola, E., Pellegrino, A., Fuggi, A., Fioretto, A., 2014. Microbial enzyme activities, fungal biomass and quality of the litter and upper soil layer in a beech forest of south Italy. Eur. J. Soil Sci. 65 (2), 274–285.
Poll, C., Brune, T., Begerow, D., Kandeler, E., 2010. Small-scale diversity and succession of fungi in the detritusphere of rye residues. Microb. Ecol. 59 (1), 130–140.
Rincón-Molina, C.I., Martínez-Romero, E., Ruiz-Valdiviezo, V.M., Velázquez, E., Ruiz-Lau, N., Rogel-Hernández, M.A., Villalobos-Maldonado, J.J., Rincón-Rosales, R., 2020. Plant growth-promoting potential of bacteria associated to pioneer plants from an active volcanic site of Chiapas (Mexico). Appl. Soil Ecol. 146, 103390. https://doi.org/10.1016/j.apsoil.2019.103390.
Romaní, A.M., Fischer, H., Mille-Lindblom, C., Tranvik, L.J., 2006. Interactions of bacteria and fungi on decomposing litter: differential extracellular enzyme activities. Ecology 87 (10), 2559–2569.
Roy-Bolduc, A., Bell, T.H., Boudreau, S., Hijri, M., 2015. Comprehensive sampling of an isolated dune system demonstrates clear patterns in soil fungal communities across a successional gradient. Environ. Microbiol. Rep. 7 (6), 839–848.
Sasmito, S.D., Kuzyakov, Y., Lubis, A.A., Murdiyarso, D., Hutley, L.B., Bachri, S., Friess, D.A., Martius, C., Borchard, N., 2020. Organic carbon burial and sources in soils of coastal mudflat and mangrove ecosystems. Catena 187, 104414. https://doi.org/10.1016/j.catena.2019.104414.
Schisler, D.A., Yoshioka, M., Vaughan, M.M., Dunlap, C.A., Rooney, A.P., 2019. Nonviable biomass of biocontrol agent Papiliotrema flavescens OH 182.9 3C enhances growth of Fusarium graminearum and counteracts viable biomass reduction of Fusarium head blight. Biol. Control 128, 48–55.
Schmidt, M.W., et al., 2011. Persistence of soil organic matter as an ecosystem property. Nature 478, 49–56.
Schneider, T., et al., 2012. Who is who in litter decomposition? Metaproteomics reveals major microbial players and their biogeochemical functions. ISME J. 6, 1749–1762.
Schostag, M., et al., 2015. Distinct summer and winter bacterial communities in the active layer of Svalbard permafrost revealed by DNA- and RNA-based analyses. Front. Microbiol. 6, 399.
Selmants, P.C., Litton, C.M., Giardina, C.P., Asner, G.P., 2014. Ecosystem carbon storage does not vary with mean annual temperature in Hawaiian tropical montane wet forests. Glob. Chang Biol. 20, 2927–2937.
Semenov, A.M., Batomunkueva, B.P., Nizovtseva, D.V., Panikov, N.S., 1996. Method of determination of cellulase activity in soils and in microbial cultures, and its calibration. J. Microbiol. Methods 24, 259–267.
Sheng, M., et al., 2017. Changes in arbuscular mycorrhizal fungal attributes along a chronosequence of black locust (Robinia pseudoacacia) plantations can be attributed to the plantation-induced variation in soil properties. Sci. Total Environ. 599–600, 273–283.
Siles, J.A., Margesin, R., 2016. Abundance and diversity of bacterial, archaeal, and fungal communities along an altitudinal gradient in alpine forest soils: what are the driving factors? Microb. Ecol. 72, 207–220.
Stone, M.M., et al., 2012. Temperature sensitivity of soil enzyme kinetics under N-fertilization in two temperate forests. Glob. Change Biol. 18, 1173–1184.
Stosiek, N., et al., 2019. N-phosphonomethylglycine utilization by the psychrotolerant yeast Solicoccozyma terricola M 3.1.4. Bioorg. Chem.
Sukdeo, N., Teen, E., Rutherford, P.M., Massicotte, H.B., Egger, K.N., 2018. Selecting fungal disturbance indicators to compare forest soil profile re-construction regimes. Ecol. Ind. 84, 662–682.
Sun, S., Li, S., Avera, B.N., Strahm, B.D., Badgley, B.D., 2017. Soil bacterial and fungal communities show distinct recovery patterns during forest ecosystem restoration. Appl. Environ. Microbiol. 83.
Tanney, J.B., Hutchison, L.J., 2010. The effects of glyphosate on the in vitro linear growth of selected microfungi from a boreal forest soil. Can. J. Microbiol. 56, 138–144.
Thuille, A., Schulze, E.-D., 2006. Carbon dynamics in successional and afforested spruce stands in Thuringia and the Alps. Glob. Change Biol. 12, 325–342.
Tischer, A., Blagodatskaya, E., Hamer, U., 2015. Microbial community structure and resource availability drive the catalytic efficiency of soil enzymes under land-use change conditions. Soil Biol. Biochem. 89, 226–237.
Tripathi, G., Deora, R., Singh, G., 2013. The influence of litter quality and micro-habitat on litter decomposition and soil properties in a silvopasture system. Acta Oecologica 50, 40–50.
Urbanová, M., Šnajdr, J., Baldrian, P., 2015. Composition of fungal and bacterial communities in forest litter and soil is largely determined by dominant trees. Soil Biol. Biochem. 84, 53–64.
Vanderhoof, M.K., et al., 2021. Tracking rates of postfire conifer regeneration vs. deciduous vegetation recovery across the western United States. Ecol. Appl. 31, e02237.
Voriskova, J., Baldrian, P., 2013. Fungal community on decomposing leaf litter undergoes rapid successional changes. ISME J. 7, 477–486.
Vormstein, S., Kaiser, M., Piepho, H.P., Ludwig, B., 2020. Aggregate formation and organo-mineral association affect characteristics of soil organic matter across soil horizons and parent materials in temperate broadleaf forest. Biogeochemistry 148, 169–189.
Wang, Q., Garrity, G.M., Tiedje, J.M., Cole, J.R., 2007. Naive Bayesian classifier for rapid assignment of rRNA sequences into the new bacterial taxonomy. Appl. Environ. Microbiol. 73, 5261–5267.
Wang, Z., Lv, J., Gu, F., Yang, J., Guo, J., 2020. Environmental and economic performance of an integrated municipal solid waste treatment: a Chinese case study. Sci. Total Environ. 709, 136096.
Waring, B.G., Adams, R., Branco, S., Powers, J.S., 2016. Scale-dependent variation in nitrogen cycling and soil fungal communities along gradients of forest composition and age in regenerating tropical dry forests. New Phytol. 209, 845–854.
Wu, Y.T., et al., 2013. Forest age and plant species composition determine the soil fungal community composition in a Chinese subtropical forest. PLoS ONE 8, e66829.
Yang, J.K., Zhang, J.J., Yu, H.Y., Cheng, J.W., Miao, L.H., 2014. Community composition and cellulase activity of cellulolytic bacteria from forest soils planted with broad-leaved deciduous and evergreen trees. Appl. Microbiol. Biotechnol. 98, 1449–1458.
Yang, Z.H., Xiao, Y., Zeng, G.M., Xu, Z.Y., Liu, Y.S., 2007. Comparison of methods for total community DNA extraction and purification from compost. Appl. Microbiol. Biotechnol. 74, 918–925.
Yuan, Z., et al., 2016. Pattern and dynamics of biomass stock in old growth forests: the role of habitat and tree size. Acta Oecologica 75, 15–23.
Zhang, D., Hui, D., Luo, Y., Zhou, G., 2008. Rates of litter decomposition in terrestrial ecosystems: global patterns and controlling factors. J. Plant Ecol. 1, 85–93.
Zhang, N., et al., 2018. Tree species richness and fungi in freshly fallen leaf litter: Unique patterns of fungal species composition and their implications for enzymatic decomposition. Soil Biol. Biochem. 127, 120–126.
Zhang, W., Wang, S., 2012. Effects of NH4+ and NO3− on litter and soil organic carbon decomposition in a Chinese fir plantation forest in South China. Soil Biol. Biochem. 47, 116–122.
Zhang, X.K., et al., 2015. Community composition, diversity and metabolic footprints of soil nematodes in differently-aged temperate forests. Soil Biol. Biochem. 80, 118–126.
Zhang, Y., et al., 2019. Soil parent material and stand development stage effects on labile soil C and N pools in Chinese fir plantations. Geoderma 338, 247–258.
Zhao, F.Z., et al., 2019. Change in soil bacterial community during secondary succession depend on plant and soil characteristics. Catena 173, 246–252.
Zhao, F.Z., et al., 2018. Changes of soil microbial and enzyme activities are linked to soil C, N and P stoichiometry in afforested ecosystems. For. Ecol. Manage. 427, 289–295.
Zheng, H., et al., 2018. Litter quality drives the differentiation of microbial communities in the litter horizon across an alpine treeline ecotone in the eastern Tibetan Plateau. Sci. Rep. 8, 10029.
Zhong, Y., Yan, W., Wang, R., Wang, W., Shangguan, Z., 2018. Decreased occurrence of carbon cycle functions in microbial communities along with long-term secondary succession. Soil Biol. Biochem. 123, 207–217.
Zhou, L., et al., 2020. Soil extracellular enzyme activity and stoichiometry in China's forests. Funct. Ecol.
Zhou, Y., Zhu, H., Yao, Q., 2018. Contrasting P acquisition strategies of the bacterial communities associated with legume and grass in subtropical orchard soil. Environ. Microbiol. Rep. 10, 310–319.
Zhu, T., et al., 2012. Nitrogen mineralization, immobilization turnover, heterotrophic nitrification, and microbial groups in acid forest soils of subtropical China. Biol. Fertil. Soils 49, 323–331.